ICAS-88-3.1.3

FRACTURE MECHANICS AND FATIGUE CHARACTERIZATION OF ALUMINIUM-LITIUM ALLOYS*

G. Cavallini, L. Lazzeri
Department of Aerospace Engineering, University of Pisa

F. Boschetti
Aeritalia Gruppo Velivoli da Combattimento, Torino

A. Solina, M. De Sanctis
Department of Chemical Engineering, University of Pisa

Abstract

With an average density about 8% lower than traditional Al alloys, the new family of Al-Li alloys is a class of materials of great interest for application in aircraft structures. These materials are now close to final definition, as far as both the chemical composition and heat treatment optimization are concerned.

Under the sponsorship of the National Research Council, many Italian aeronautical industries and University Institutes and Departments have embarked on a vast research programme for the evaluation of the main characteristics of such alloys. This programme comprises a large variety of tests, such as: static and fatigue tests, crack propagation tests, fracture toughness, stress corrosion susceptibility and exfoliation corrosion.

The paper describes the results of the fatigue tests carried out on both notched and unnotched specimens, under CA loading (R=0.1). The influence of different ageing on fatigue behaviour and the metal structure was also assessed in certain cases. The results are also given of crack propagation tests, both under CA loading and FALSTAFF spectrum, and of fracture toughness tests, which allow evaluation of the damage-tolerance properties. With the aim of a better assessment of the capabilities of these materials, a comparison with traditional alloys was carried out by means of an example of application of the data obtained to the fatigue design of a typical structure, a lower wing stiffened panel.

1. INTRODUCTION

Starting from the pioneering era at the beginning of the century up to the present time, the evolution of materials and that of the types of structural solutions utilized in aircraft construction have gone hand in hand. In the days of the Wright brothers, wood, cotton fabric and ropes were the main materials available and biplane was the typical architecture. The development of Al-Cu alloys (first produced in 1909) led gradually to the cantilever monoplane with an all-metal monocoque construction, the most common architectural solution since the thirties. The application of aluminium cladding and the development of high-strength Al-Zn alloys were the two major milestones in the development of aluminium industry in World War II, while in recent decades an increasing demand for good fatigue performance and a high toughness has fostered the development of damage-tolerant alloys. In even more recent times, the introduction of advanced composite materials in aircraft construction has revolutionized the approach to the problem of material selection. Predictions about their use in modern aircraft, designed for the '90s and beyond, are of about 50% of total structural weight for tactical military airplanes and about 30% for commercial aircraft. The increasing use of advanced composite materials has helped to speed up the natural development of new advanced aluminium alloys by the metallurgy industry.

In this general situation, the so-called new Al-Li alloys occupy an important position; they differ from the traditional Al-Cu or Al-Zn alloys because of the presence of Litium, in quantities of about 2-3% in weight, as the first or second alloying element. As a result of its very low density, it follows that, for each 1% in weight of Li added to a traditional Al alloy, a global specific weight of about 4% is obtained. This is achieved by substituting heavier reinforcing elements (e.g. Cu and Zn precipitates) by much lighter Al-Li compounds. A very interesting feature of Al-Li alloys, from the point of view of aircraft construction, is the fact that no special equipment or tooling investment are required, as in the case of composite materials. Besides, classical design and manufacturing techniques can be maintained, as well as established airline maintenance (and repair) practices.

Therefore, in this reference situation, the most important aluminium alloy manufacturers have invested extensively, in terms of financial and human resources, in research and in the development of Al-Li alloys with not only low density features, but also mechanical and workability characteristics

* This work was partly financed by the Italian National Research Council.

suitable for use in the aircraft industry.

In the last decade, a number of Li-based Al alloys have been developed by the main industries and some of them have already been registered. The alloys that have reached an advanced stage of development and are almost ready for commercialization are 2090, 2091 and 8090. Each of these has a different target alloy which it is intended to substitute:

a) 2090 is a high-strength alloy, mainly developed to replace 7075-T6. As a consequence of market demand, a series of tempers has been developed in order to obtain different specific properties.

b) 2091 was developed to obtain medium strength and good toughness properties; it seems likely to replace 2024-T3 in the proper temper conditions.

c) the target of 8090 is quite similar to that of 2091, but with higher static properties. According to the heat treatment, it is likely to replace either 2024-T3 or 2014-T6.

Besides the objective of obtaining the overall properties which are typical of the alloys to be substituted (static and fatigue strength, toughness, corrosion resistance, crack propagation behaviour, etc), all these alloys have another interesting feature: their elastic modulus is almost 10% higher than that of the conventional Al alloys.

At the current research and development level of the products, evaluation programs are being carried out by the aircraft manufacturing industry and research institutes. This paper contains the results of research aimed at assessing the fatigue and damage-tolerance properties of certain Al-Li alloys, carried out by Aeritalia-GVC (Gruppo Velivoli Combattimento) and by the Departments of Aerospace Engineering and Chemical Engineering of the University of Pisa. Some of the results are the property of Aeritalia, to whom the Authors are grateful for allowing publication. Other results were obtained within the framework of a research program, still in progress, which is financed by the Italian National Research Council (C.N.R.) and which coordinates research carried out by both industries and Universities.

2. EXPERIMENTAL PROGRAM

The following producers supplied batches of suitable Al-Li material are: Alcoa, British Alcan and Cegedur Pechiney. The alloys examined were 2090, 2091 and 8090, in different thicknesses and, in certain cases, also in different heat treatments or in overaged conditions. This paper only contains the results of fatigue tests performed on notched and unnotched specimens and of fatigue crack propagation and fracture toughness tests. No discussion will be found here of all the other kinds of experimental activities included both in the Aeritalia and in the C.N.R. assessment programs (static, corrosion resistance, formability, etc).

Fatigue tests were carried out on plain specimens, whose geometry is shown in Fig. 1 (Kt = 1.07, /1/); the same geometry was used for the notched specimens, when a hole, 5 mm in diameter, was simply drilled at the center (Kt = 2.5 referred to net area, /1/).

For many batches of material, fatigue tests specimens were prepared both in the L and LT direction. Due to the preliminary nature of the investigation, fatigue tests were carried out under constant amplitude axial loading, with a stress ratio R (=Smin/Smax) equal to 0.1. Crack propagation tests were carried out mainly under constant amplitude loading, characterized by different stress ratios, but preliminary tests under FALSTAFF spectrum loading, /2/, were also performed.

The Department of Chemical Engineering of the University of Pisa cooperated in the program by carrying out sample fractography by using a JEOL T300 SEM and structural characterization of materials by means of Transmission Electron Microscopy.

3. FATIGUE TEST RESULTS

The fatigue test results will be presented separately for each material. Certain observations can be made which hold good for all the materials. The presence of Litium, a highly reactive element, causes quick oxidation of the fracture surfaces; therefore timely dismounting of the failed specimen from the fatigue machine and gold coating are necessary, in order to ensure surface readability in subsequent metallographic analysis.

Fatigue test results have been compared with data from MIL-HDBK-5D, but personal experience is that quite often the actual fatigue behaviour of a material is somewhat lower than expected according to MIL-HDBK-5D data.

2091 Alloy

The target of this alloy is medium strength and good fatigue properties. The typical chemical composition is shown in Table I; the average density is 2.57. Three thicknesses were available: 1.6 mm and 3.0 mm sheets and 12.0 mm plate. The three materials, all from the same manufacturer, were also in different heat treatments:

t=1.6 mm: -T6
t=3.0 mm: -T8
t=12.0 mm: -T651.

The three heat treatments were different and produced different properties in the material. Nevertheless, the results obtained from the different batches will be compared in the following, without showing conspicuous differences.

Fig. 2 contains all the results from unnotched specimens. It shoul be noted that no particular influence can be ascribed to thickness (the data is almost uniformly distributed; the behaviour of the smaller gages is no better, as expected; a certain amount of contradictory behaviour can be observed) or to the principal lamination direction. Comparison with the reference material, 2024-T3, from MIL-HDBK-5D, shows poor fatigue behaviour: for

equal life, the reduction in stress is about 20%.

It is difficult to draw definite conclusions from examination of the data in Fig. 2, due to the existence of contradictory tendencies and a certain amount of non-homogeneity in the batches (different heat treatments, effect of thickness, effect of grain orientation), which can interfere with each other. A rather wide scatter is also observed.

Another batch of material, 2091-T3, 1.6 mm thick, was made available by another manufacturer. Only L specimens were made and tested; Fig. 3 contains a comparison between the two manufacturers, for the same thickness and grain orientation. The material of the second producer proved to be of a much higher quality and with better characteristics: for equal life, the reduction in stress as compared to the traditional alloy is only 10% in the low number of cycles, and the fatigue limit seems to be very similar.

Fig. 4 shows the results of fatigue tests carried out on notched specimens, made from 1.6 mm sheet material and from plate 12.0 mm thick. The stresses are referred to the gross area. The material is the same as that used for the unnotched specimens in Fig. 2. The results are well grouped, independently of thickness and the principal grain direction. Comparison with data in the literature concerning the 2024-T3 alloy (Kt=3.4, gross area) shows lower fatigue strength, even for notched specimens; in this case, too, the reduction in stress for equal life is about 20%.

8090 Alloy

This alloy is conceived for general purpose: medium strength and good fatigue and damage-tolerance properties, according to the heat treatment. The average chemical composition is given in Table I. Litium is the first alloying element with a weight percentage of about 2.3-2.6%, thus resulting in an average density of about 2.54 gr/cc. Only one manufacturer supplied batches of material: thicknesses were 1.6 mm and 3.0 mm. The heat treatment was -T6, but for 1.6 mm sheet a small quantity of the -T651 condition was also available, from which only unnotched L fatigue specimens were obtained. Only plain specimens were prepared, due to the small quantity of material available, and the results are shown in Fig. 5. A certain amount of contradictory behaviour is observed: LT specimens proved to possess a slightly better fatigue strength, as well as greater thickness. The behaviour of the T651 sheet specimens was consistent with the T6 material, but the points fall mainly in the lower part of the scatter band.

Anyway, for this material, too, the comparison with the handbook properties of traditional alloys is unfavourable, to the usual extent of about 20% in stress.

2090 Alloy

This is a rather different alloy from the previous ones: it is aimed at achieving the high strength characteristics of the 7075-T6 alloy with a density reduction of about 8%. In response to a market demand for other property combinations, a series of tempers were developed. The material made available was in the -T8E41 condition, which is the temper that most closely approximates the overall properties of 7075-T6. Three thicknesses were available: 1.6 mm, 3.3 mm and 12 mm, from a single manufacturer. Plain specimens were built with this alloy, in the L and LT directions, with the exception of the LT direction for the 1.6 mm material. The results are shown in Fig. 6, compared with 7075-T6. In this case, too, the fatigue strength of the Al-Li alloy is lower than that of the traditional alloy, but to a considerably lesser extent than the other alloys. Taking into account the fact that the effective stress concentration factor of plain specimens is 1.07, it may be stated that the aim of obtaining the same fatigue properties as in the case of 7075-T6 has been achieved. It should be noted that the behaviour is the same in both directions L and LT, and also for different thicknesses. The only observation that needs to be made concerns the particularly poor fatigue strength of the L specimens 3.3 mm thick which, however, may be ascribed to surface defects, in the form of small pitting.

Fatigue tests were carried out on overaged material from the plate, subjected to 10 hours and 100 hours at 125 °C. The results do not show a particular change in fatigue behaviour. The 3.3 mm material was also subjected to an overaging treatment of 100 hours at 135 °C. The results are shown in Fig.7.

Notched specimens were prepared from the plate and from 1.6 mm sheet. Comparison with data in the literature concerning 7075-T6, available for Kt=3.4, is interesting: it shows that the fatigue strength is quite similar (Fig. 8). Curiously enough, the LT direction produced better results than the L direction. Anyway, the fatigue properties of 2090-T8E41 do not seem to be inferior to those of the alloy to be substituted (7075-T6).

4. FRACTURE MECHANICS TESTS RESULTS

Determination of fatigue crack propagation behaviour and fracture toughness is important for the evaluation of a new material, because these are fundamental properties for the design of damage-tolerant structures. Therefore, fatigue crack propagation tests were planned, both under Constant Amplitude (CA) loading and under flight-by-flight spectrum, using the FALSTAFF standard sequence. Center cracked tension specimens were used for these tests. According to the material available, two kinds of specimen geometries were used: the first one was 120 mm wide and the second one 400 mm. This last specimen was used for the fracture toughness tests. The notch at the center of the specimen was made by means of a jeweller's saw. The test results were analyzed by means of standard

programs developed by the Department of Aerospace Engineering and based on the use of spline functions for the numerical determination of the crack growth rate.

4.1 - Crack propagation results

2091 alloy

CA tests were carried out on 2091-T8 material, available from one manufacturer in two thicknesses, 3 mm and 1.6 mm thick, respectively.

The first material was evaluated, using 120 mm wide CCT specimens. Ten specimens were tested by applying the load in the L direction, at different stress ratios (Smin/Smax), (R= -0.2, 0., .2 and .5) and six specimens were tested in the LT direction (R= -0.2, 0. and 0.4). The average initial crack length was 6 mm. Some of the results of the L specimens are summarized in a da/dn-ΔK plot in Fig. 9 and those of the LT specimens in Fig. 10. In both figures, for comparison, some typical results of 2024-T3 Alclad, from /3/, are also shown, but they are relevant to a thinner material (1 mm). From this comparison it can be deduced that the crack propagation properties of 2091 are comparable to those of the best aeronautical alloys, at least in the range of high ΔK values. Besides, the characteristics in the LT direction seem even slightly better than in the L direction.

Only three specimens of 2091-T8, supplied by the same manufacturer, were available for the 1.6 mm thickness; they were 400 mm wide and all in the L direction. They were tested under CA loading, with R values of 0.1 and -0.2 (Fig. 11). Comparison with the same nominal material, 3 mm thick, shows much better behaviour, specially at intermediate ΔK values.

Another manufacturer supplied sheets of 2091, 1.6 mm thick, in the T3 condition (same material as the one in Fig. 3); 400 mm wide specimens were prepared and tested under CA loading, in the L direction. The results are plotted in Fig. 12, which shows substantial improvements in performance, specially at positive stress ratios.

Crack propagation tests were also carried out under flight-by-flight spectrum loading, namely the FALSTAFF sequence, to assess if the interaction effects between load cycles of different amplitude were similar to those occurring in traditional Al alloys. The tests were carried out on specimens of 2091-T8, 3 mm thick and 120 mm wide (same batch as the one of CA tests, Figs. 9-10); two values of maximum stress in the spectrum were used: 196 MPa and 235 MPa. The test results were analyzed in terms of da/df (average crack growth rate per flight, evaluated by means of the incremental ratio) versus Kmax (evaluated by relating the maximum stress in the spectrum to the average crack length in the growth interval being considered). Comparison with results obtained on 2024-T3 Alclad in research carried out at the Pisa Department of Aerospace Engineering, /4/, shows quite similar behaviour, i.e. it confirms the conclusions that had been drawn on the basis of CA tests, /5/.

8090 Alloy

This alloy was supplied by the manufacturer in two thicknesses, 1.6 mm and 3.0 mm; they were both in the T6 condition. Crack propagation tests under CA loading were carried out on 400 mm wide specimens, in the L direction. The limited amount of material available allowed us to perform only three tests. Preliminary assessment of this research suggested it would be betterto use only one value of stress ratio, namely R=0.1. Due to a trivial mistake in the test procedure, data was obtained in the intermediate-high ΔK range. However, the results in Fig. 13 show a slight influence of thickness on the crack propagation rate, consistent with the expected trend. Bearing in mind that heat treatment T6 is not specifically designed for damage tolerance, the results show interesting characteristics of 8090-T6, in no way inferior to those of the traditional 2024-T3.

On the basis of the few results obtained, 8090-T6 seems to have intermediate crack propagation characteristics which are somewhere between those of the traditional 2024-T3 and those, even better, of 2091.

2090 Alloy

This material was supplied by the manufacturer in the T8E41 condition, which is the temper that most closely approximates the overall 7075-T6 properties. Three specimens, 1.6 mm thick and 400 mm wide, were tested under CA loading with the load applied in the L direction. The results are shown in Fig. 14, together with reference data obtained at the Pisa Department of Aerospace Engineering on 7075-T6, 1 mm thick, R=0.06, /6/. The improvement in crack resistance is considerable.

4.2 - Fracture toughness results

For those materials, for which sufficiently wide specimens (i.e. 400 mm) were available, fracture toughness was evaluated at the end of fatigue crack propagation. The following average values of Kc were obtained:

2091-T8, t=1.6 mm: ---> Kc = 103 MPa*sqrt(m)
2091-T3, t=1.6 mm: ---> Kc = 106 "
8090-T6, t=1.6, 3 mm: ---> Kc = 70 "
2090-T8E41, t=1.6 mm: ---> Kc = 43 "

All the results are relevant to the L direction.

These results are interesting, because the following values were obtained in tests carried out at the Pisa Department of Aerospace Engineering /7/ for traditional alloys:

2024-T3, t=1.0 mm: ---> Kc = 98 MPa*sqrt(m)
7075-T6, t=1.0 mm: ---> Kc = 68 "

The damage-tolerant alloy 2091 shows a high toughness, i.e. considerable capability to carry loads in the presence of defects. The value obtained, specially for the T3 condition, must be considered as a lower limit of the actual characteristics, because the width of 400 mm of the panels proved to be inadequate for this material, according to the Feddersen theory, /8/.

On the contrary, the value obtained for 2090-T8E41 is very low and anyway much less than the comparison material, 7075-T6.

5. OPTICAL AND ELECTRON MICROSCOPY

Microstructural observations were carried out on most materials here studied, by using both optical and electron (SEM, TEM) microscopy. In the following, a brief description of the main results is summarized.

5.1 - TEM observations

Figs. 15 a,b show the structure of 2091-T8 alloy which appears underaged, as confirmed by the high density of helical and loop dislocations and by reduced dimensions of δ' (Al_3 Li) spherical particles. Moreover, S' metastable phase (Al_2CuMg), typical age-hardening product of Mg-containing alloys, is practically absent.

The secondary phase precipitation in 8090-T6 alloy is mainly constituted by coarsened δ' particles (Figs. 15 c,d), with a low density of S' and T1 (Al_2CuLi) precipitates, which could be inferred from the absence of prestretching in T6 condition.

According to differences in chemical composition and age hardening treatments, the presence of θ' (Al_2 Cu, AlCuLi) and T1 metastable phases is observed in 2090-T8E41 in addition to δ' particles, as shown in Figs. 15 e,f. Following overaging 100 hours at 125°C, a higher density of all plate-like precipitates (θ' and T1) was observed, together with a coarsening of spherical δ' particles, Figs. 15 g,h. Finally, only for these heat treatment conditions, evidence has been revealed for gb precipitate free zones of reduced width, with formation of stable phases at gb.

5.2 - SEM and optical observations

The fractographic analysis was carried out mainly on 2091-T8 and 2090-T8E41 alloys, highlighting the different mechanisms which influence fatigue and static fracture of the two materials.

The macrographic examination of the fatigue failed specimens of 2091-T8 alloy showed a crack propagation orthogonal to the direction of applied load; this feature occurred both in fatigue and, as a general trend, in static fracture regions, Fig. 16a. Cracks usually nucleated on the short side of the specimens, presumably in presence of defects (mainly inclusions); morphology appeared homogeneous all over the area. Fracture surfaces of 2090-T8E41 alloy, on the contrary, were characterized by a typical slaty appearance, particularly evident for the thickest material (12 mm plate) and in overaged treatment conditions, Figs. 16b,c. In this case, cracks nucleated on the long side of specimens and propagation occurred, also in the fatigue growth area, along a direction noticeably inclined with respect to the orthogonal direction to the load.

The optical microscopy observation reveals an almost complete recrystallization of 2091-T8 alloy, with a typical grain size of about 20-40 μm, Fig. 17a; the structure of 2091-T3 alloy, provided by a different producer, differs from the previous one for a less complete recrystallization, and for a less pronounced presence of inclusions, which are also of reduced dimensions. In 2090-T8E41 alloys, the grains are strongly elongated in the rolling direction, Figs. 17b,c and their transverse dimension is higher in value for the plate (average, 12 μm) with respect to the sheet (average, 4 μm). Moreover, in this material, high angle grain boundaries exhibited a strong response to the etchant, probably associated to the presence of gb precipitates.

The reason of such a differentiation in the macrographic aspect of fractures between 2091-T8 and 2090-T8E41 fatigue failed specimens were observed more clearly by SEM fractography. For the first material, the fatigue failure zone is characterized by the presence of typical growth lines, with formation of ductile dimples in correspondence to intermetallic inclusions; in the second material, in addition to areas similar to those described above, many areas of rapid propagation were observed. However, most noticeable differences occur in regions of static fracture. In 2091-T8 alloy, the static fracture is essentially transgranular with presence of slip bands and, again, many dimples formed around intermetallic particles, Fig. 18. On the contrary, in 2090-T8E41 alloy, the static fracture propagates on planes both orthogonal and parallel to the applied load: along the orthogonal direction, the fracture appeared transgranular, Fig. 19, whereas along the parallel direction it was mainly intergranular with formation of a high density of microdimples, which appear of larger dimension for the overaged alloy condition, Figs. 20 and 21. Dimples due to intermetallic inclusions were frequently present only in regions close to the surface of 3.3 mm sheet.

6. IS IT CONVENIENT TO INTRODUCE AL-LI ALLOYS IN AIRCRAFT CONSTRUCTION?

The properties of Al-Li alloys, discussed in the present paper, were compared with those of traditional alloys by applying them, for the sake of example, to the problem of fatigue-sizing of a lower wing stiffened panel of a transport aircraft. In this application, simplified durability and damage-tolerance requirements had to be complied with.

The materials examined were 2024 and 2091 for the skin and 7075 and 2090 for the stringers. Since this application was merely an example, many simplifying assumptions were made:

(i) the geometry and spacing of the stringers and the panel width were considered a datum of the problem;

(ii) the only dimension to be defined was that of skin thickness;

(iii) the load spectrum was simplified: from the point of view both of durability and damage-tolerance, each flight was considered to be equivalent to two cycles with R=0; these are a sort of Ground-Air-Ground cycles reduced in range as far as the minimum stress is concerned, because real GAG cycles are typically characterized by negative values of R.

(iv) the maximum load sustained by the panel in a flight was assigned;

(v) the durability objective assumed was a crack-free life of 20000 flights;

(vi) the damage-tolerance requirement was to ensure safety through scheduled inspections every 5000 flights with a NDI method that allows confident detection of cracks 3 mm long.

The procedure for sizing the skin thickness consists in evaluating the maximum stress allowed by the durability target (therefore deriving the minimum skin thickness required) and then to perform Fracture Mechanics analysis to check the compliance with the damage-tolerance requirement.

This application requires knowledge of B-basis fatigue curves, i.e. the curves representing 90% survival probability with a 95% confidence level. The fatigue data obtained was statistically analysed in order to evaluate the average curve and the standard deviation, which, through the application of the appropriate reliability coefficient that is a function of the number of tests, allows us to define the 90/95 S-N curve. Mean curves of traditional alloys were taken from MIL-HDBK-5D, while values of standard deviations were taken from the literature. The S-N curves of Al-Li alloys were relevant to Kt=3.125, which is rather low when it comes to representing the stress concentration factor of a hole with a rivet transferring load. However, this difference was consided to be relatively unimportant in this application, as was the difference in the stress ratio (the data for Al-Li alloys is relevant to R=0.1 and not R=0).

The durability requirement was complied with through the use of S-N curves, which provided the allowable average stress in the section for the prescribed number of cycles (40000); this stress allows us to assess the minimum skin thickness. Compliance with the damage-tolerance requirement was verified through assessment of the stress intensity factor in relation to crack length. This was done by means of the Poe approach /9/, modified to take the bending stiffness of the stringer into account. The behaviour of the rivets was assumed to be rigid. In this way, a simple linear crack propagation analysis was carried out, which allowed us to check that critical dimensions would not be reached before 20000 cycles (two inspection intervals), assuming that the initial defect was a crack emanating 1.40 mm out of a rivet hole. The fail-safe load which had to be sustained by the cracked structure was assumed 1.6 times higher than the maximum load in a flight. The Forman law was used; in the case of the 2091 alloy, the data from T8 material was used. The integrity of the stringer for the prescribed number of cycles was checked both for static loads and for fatigue loading. The load transferred from the cracked skin to the stringer was evaluated with the Poe approach and Miner linear cumulative damage analysis was performed to check the fatigue strength of the stringer.

Most of the simplifying assumptions made in the example are shown in Fig. 22. The minimum skin thickness values obtained from the example are summarized in the following:

	Durability	Damage Tolerance
2091-T8	1.06 mm	0.9 mm
2024-T3	0.59 mm	1.3 mm

Therefore the following dimensions satisfy both requirements:

skin 2091/stringer 2090 ---> 1.06 mm/1.0 mm

skin 2024/stringer 7075 ---> 1.30 mm/1.0 mm.

Comparison of the weights is in favour of the Al-Li solution: a reduction in weight to 79.7% is observed. It is interesting to note that, if the damage tolerance requirement alone had to be complied with, the weight would have dropped to 71.8%; on the contrary, if the durability requirement alone is considered, an increase in weight of 28.2% occurs.

These results look interesting, though they refer to a greatly simplified example. Anyway, the durability and damage-tolerance requirements were rather realistic and it is felt that, for requirements not much different from those of the example, the results will be quite similar. Therefore, for appropriate structures, whose dimensions depend on compliance with damage-tolerance requirements, lighter solutions are likely to be obtained.

7. CONCLUSIONS

In the present paper many results concerning fatigue and the Fracture Mechanics characterization of available Al-Li alloys have been given; they must still be considered as preliminary, because these materials are still in the final stage of development. Alloy 2090 is the nearest to being commercially available on an industrial basis. From these results, the following conclusions can be drawn:

(a) fatigue behaviour does not yet seem to be adequate, compared with data from MIL-HDBK-5D. Anyway, 2090 substantially equals the fatigue performance of the substitution alloy, while for 2091 and 8090 lower stresses are required for equal life.

(b) the crack-propagation characteristics seem

excellent: all three alloys prove to be a substantial improvement on the traditional alloys.
(c) fracture toughness is adequate for the 2091 alloy while further work is necessary for 8090 and even more for 2090.
(d) an application of the data obtained to the design of a lower wing stiffened panel shows that, in the case of structures whose sizing is governed by damage-tolerance requirements, interesting weight-saving can be obtained.

In the present paper, only fatigue and Fracture Mechanics characteristics have been examined. It should be borne in mind that the static strength is comparable to that of traditional alloys while the elastic modulus is about 8-10% higher. Besides, notwithstanding the high reactivity of Litium, corrosion susceptibility does not seem to be a problem and traditional surface finishes can be applied with satisfactory results, /10/. All these features seem to lead to the conclusion that application of Al-Li alloys in aeronautical programs will soon take place, but some open questions still exist.

It must be pointed out that weight-saving is not the right parameter for assessing a material with a view to application in commercial aircraft structures: Direct Operative Cost is the real parameter and therefore the current high cost of Al-Li alloys (about three times the price of conventional alloys) together with a low fuel price drastically reduces their cost effectiveness. Therefore, it is difficult to make predictions, even if their mechanical properties seem attractive, and only the future will provide definite answers on the real possibilities of application of Al-Li alloys in aeronautical programs.

ACKNOWLEDGEMENT
The authors wish to thank Mr. S. Giaconi, a post-graduate student, for assistance in the tests and in the analysis of the results.

REFERENCES

/1/ - Peterson R.E.: 'Stress concentration design factors', J. Wiley and Sons, N.Y., 1953.

/2/ - Anon.: 'Description of a fighter aircraft loading standard for fatigue evaluation, FALSTAFF', joint report of F+W (CH), LBF (GER), NLR (NL) and IABG (GER), March 1976.

/3/ - Lanciotti A., Lazzeri L.: 'Problematiche di fatica in campo aeronautico: alcune attività svolte presso il Dipartimento di ingegneria Aerospaziale dell'Università di Pisa', presented at the 2nd Meeting 'New Technologies for Vertical Flight', Lugo di Romagna, May 1988.

/4/ - Salvetti A., Cavallini G., Lazzeri L.: 'Fatigue crack growth under variable amplitude loading in built-up structures', Final technical report, European Research Office, United States Army, London, April 1982.

/5/ - Lazzeri L., Boschetti F., Rossi L., Solina A.: 'Valutazione delle caratteristiche della meccanica della frattura e del comportamento a fatica di leghe alluminio-litio', presented at the IX National Congress of Italian Association of Aeronautics and Astronautics (AIDAA), Palermo, October 1987.

/6/ - Lazzeri L.: 'Risultati delle prove di propagazione della fessura su pannelli piani non irrigiditi di cui alla AEPE n. 52062005 emessa dalla Soc. Aeritalia di Napoli', DDIA 83-8, Sept. 1983, Pisa Dept. Aerospace Engineering.

/7/ - Frediani A.: 'Risultati delle prove di resistenza statica residua su pannelli piani non irrigiditi di cui alla AEPE n. 52062003 emessa dalla Soc. Aeritalia di Napoli', DDIA 83-3, July 1983, Pisa Department of Aerospace Engineering.

/8/ - Feddersen C.E.: 'Evaluation and prediction of the residual strength of center cracked tension panels', ASTM STP 486, 1971, pp. 50-78.

/9/ - Poe C.C.Jr: 'Stress intensity factor for a cracked sheet with riveted and uniformly spaced stringers', NASA TR R-358, 1971.

/10/ - Leonard R.W.: 'New developments in aluminium alloys and aluminium structures', Douglas paper 8073, May 1988.

Alloy	Li	Cu	Mg	Zr	Zn	Ti	Mn	Cr	Fe	Si	Al
2091	1.7-2.3	1.8-2.5	1.1-1.9	.04-.16	.25	.10	.10	.10	.30	.20	rem.
8090	2.3-2.6	1.0-1.4	.5-0.9	.10-.14	.25	.10	.10	.10	.30	.20	rem.
2090	1.9-2.6	2.4-3.0	.25	.08-.16	.10	.15	.05	.05	.12	.08	rem.

Table I - Chemical composition of the main Al-Li alloys.

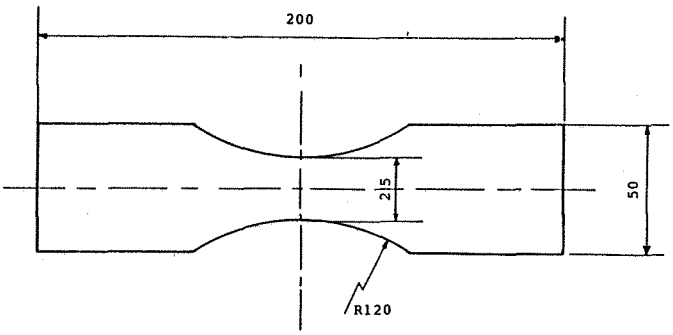

Fig. 1 - Fatigue test specimen geometry.

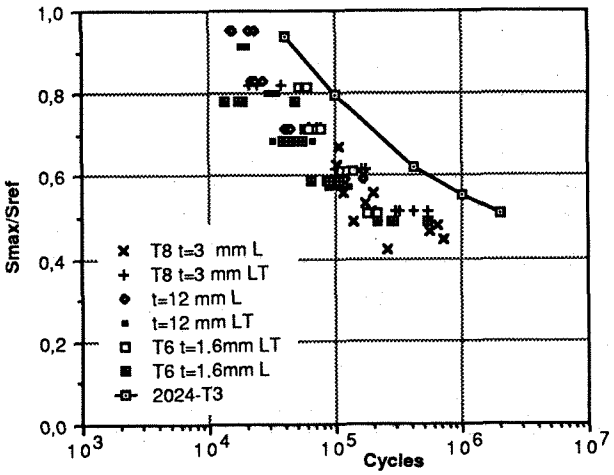

Fig. 2 - Fatigue test results of unnotched specimens, 2091. Sref = 450 MPa.

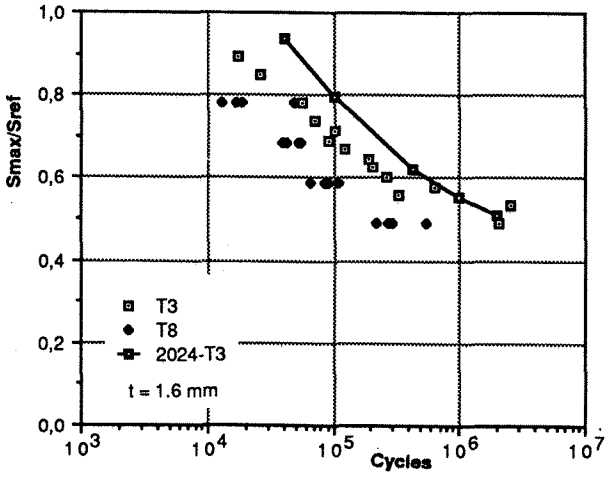

Fig. 3 - Comparison of test results of batches of 2091 made by different manufacturers. Sref = 450 MPa.

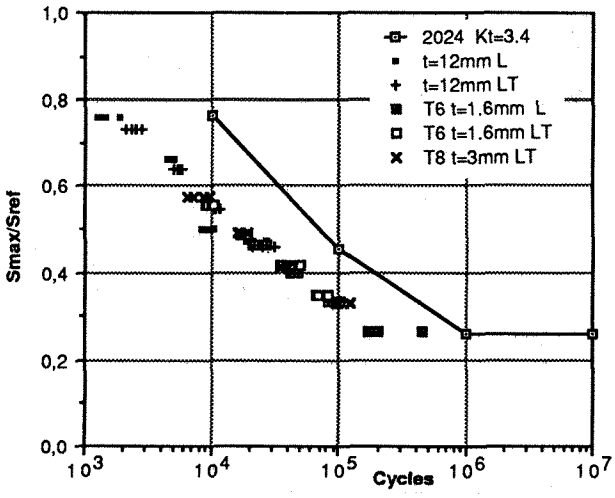

Fig. 4 - Fatigue test results of notched specimens (Kt=3.1), 2091. Sref = 450 MPa.

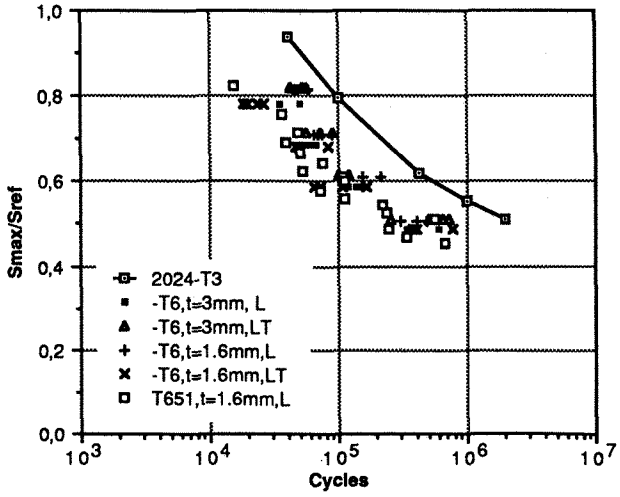

Fig. 5 - Fatigue test results of unnotched specimens, 8090. Sref = 450 MPa.

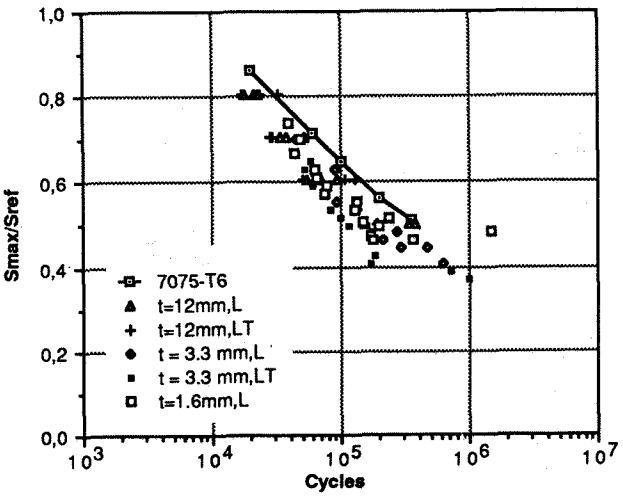

Fig. 6 - Fatigue test results of unnotched specimens, 2090-T8E41. Sref = 540 MPa.

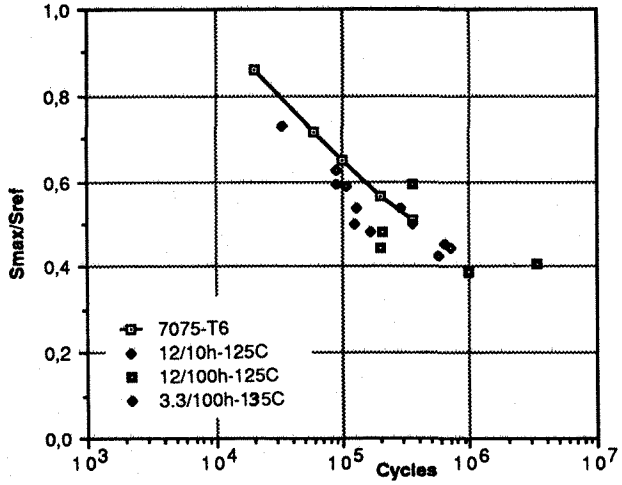

Fig. 7 - Fatigue test results of unnotched specimens, 2090-T8E41, overaged, L. Sref=540 MPa

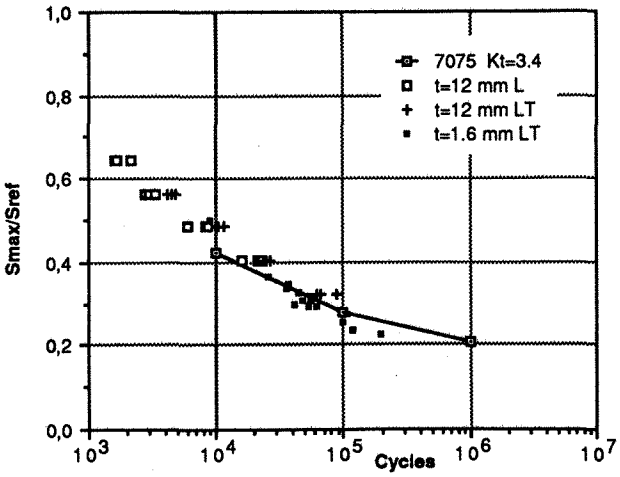

Fig. 8 - Fatigue test results of notched specimens (Kt=3.1), 2090-T8E41. Sref = 540 MPa.

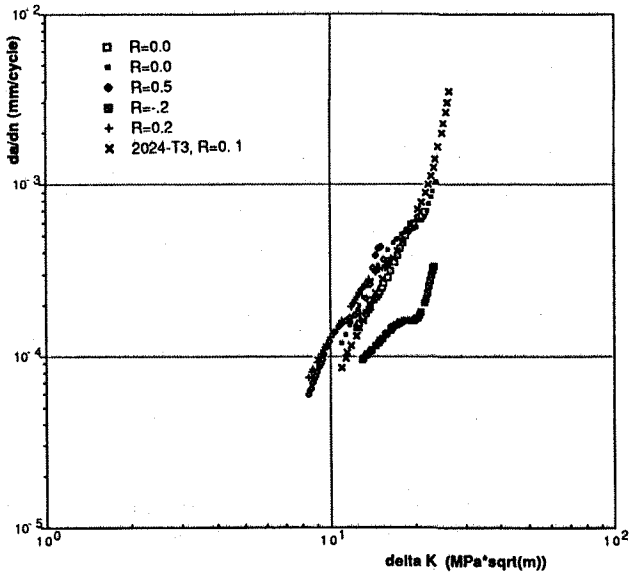

Fig. 9 - Constant amplitude crack growth data for 2091-T8, 3mm thick, L/T.

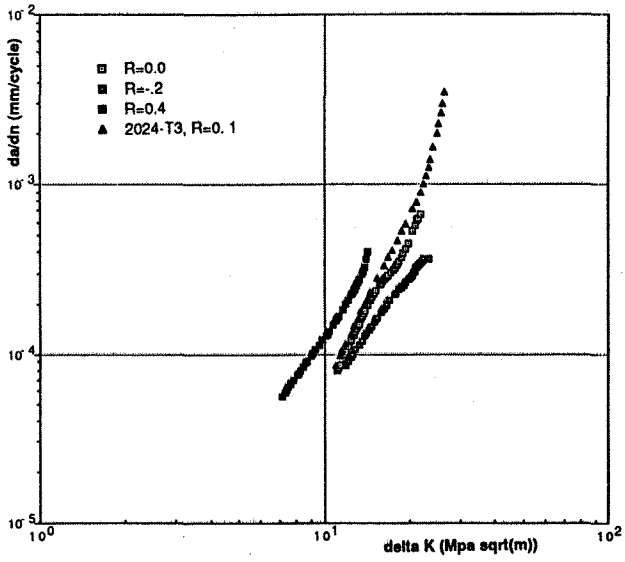

Fig. 10 - Constant amplitude crack growth data for 2091-T8, 3mm thick, T/L.

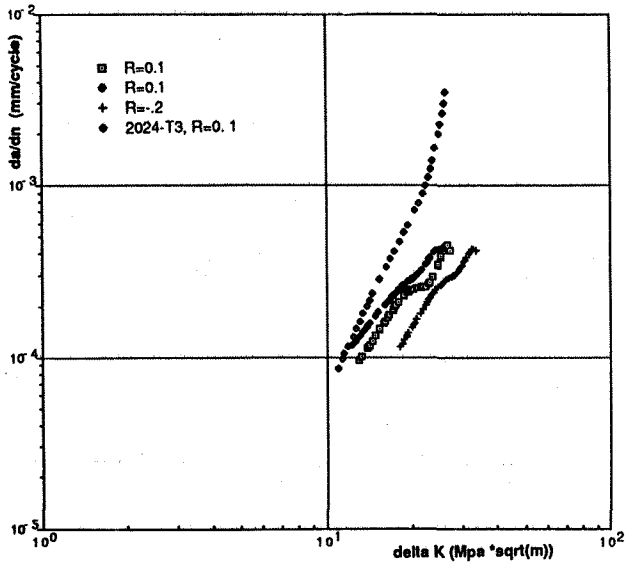

Fig. 11 - CA crack growth in 2091-T8, 1.6mm, L/T.

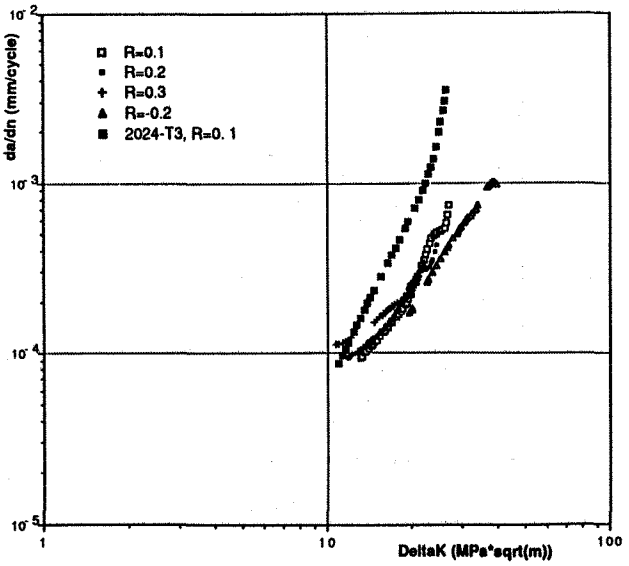

Fig. 12 - CA crack growth in 2091-T3, 1.6mm, L/T. Second manufacturer.

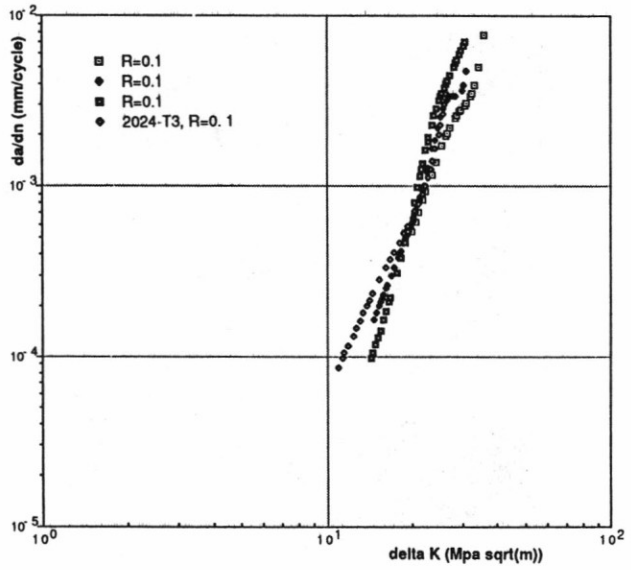

Fig. 13 - Constant amplitude crack propagation data for 8090-T6, L/T.

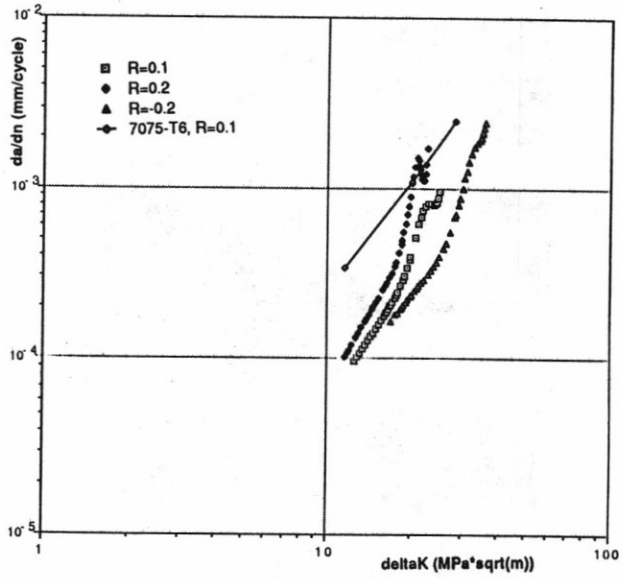

Fig. 14 - Constant amplitude crack propagation data for 2090-T8E41, 1.6mm thick, L/T.

a) b) c)

Fig. 16 - Optical macrographs of fatigue failed samples; a) 2091-T8, 3mm; b) 2090-T8E41, 3.3 mm; c) 2090-T8E41, 12mm, overaged 100 hours at 125°C.

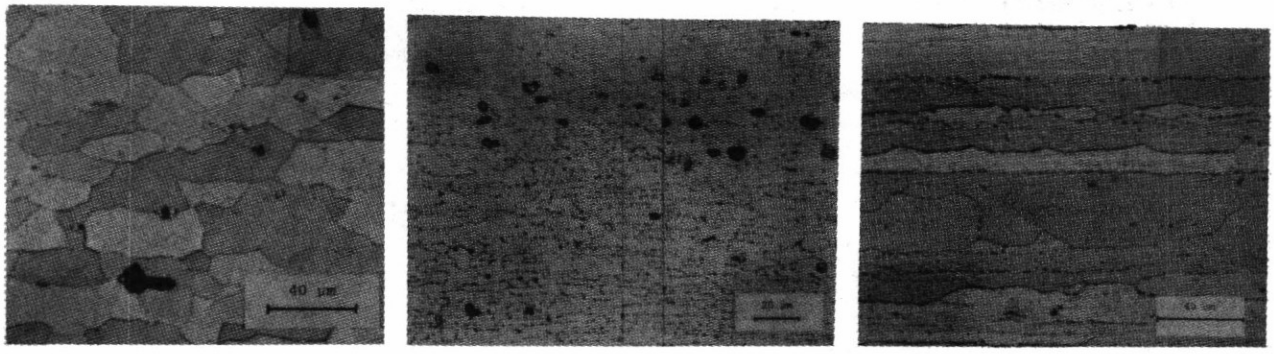

a) b) c)

Fig. 17 - Optical micrographs from longitudinal cross-sections; a) 2091-T8, 3mm; b) 2090-T8E41, 3.3mm; c) 2090-T8E41, 12 mm.

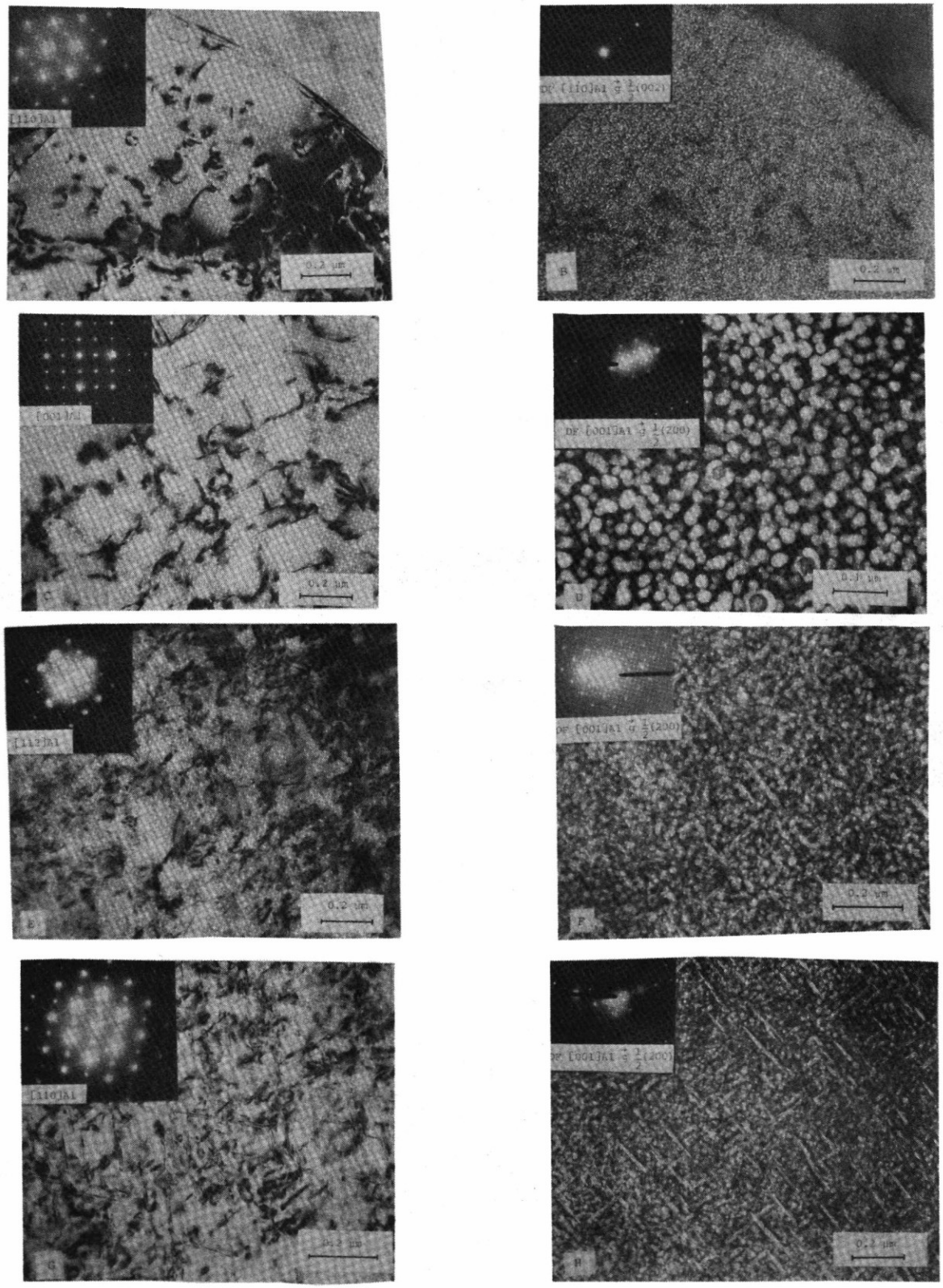

Fig. 15 - Typical TEM micrographs showing precipitate types from:
a,b) 2091-T8 alloy ---> δ' c,d) 8090-T6 alloy ---> δ' + S' + T1
e,f) 2090-T8E41, 12mm ---> δ' + θ' + T1 g,h) as before, overaged 100h/125°C ---> δ' + T1 + θ'

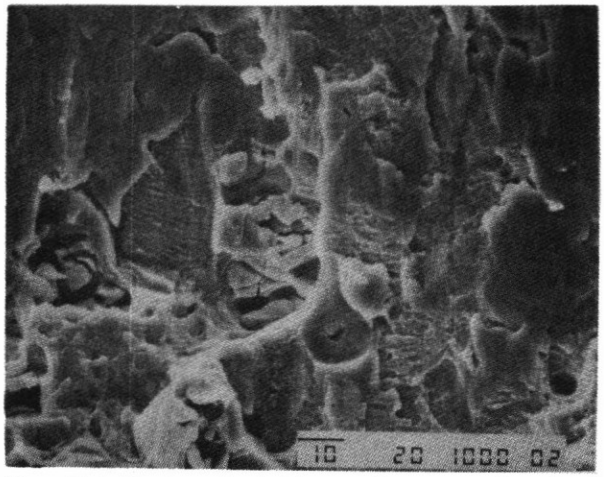

Fig. 18 - Region of static crack propagation (SEM) in 2091-T8 alloy.

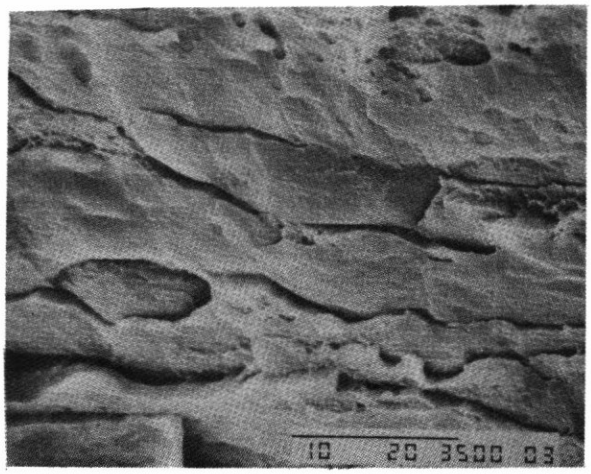

Fig. 19 - Transgranular crack propagation (SEM) along the orthogonal direction to load application in 2090-T8E41.

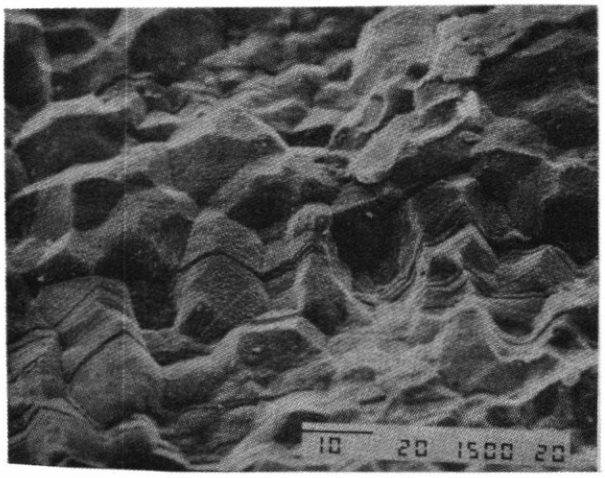

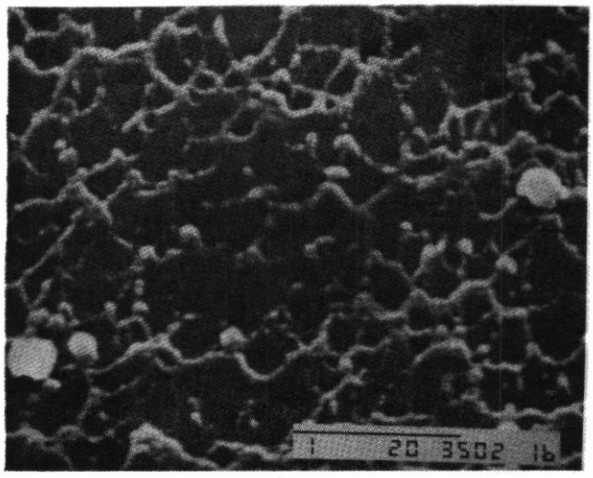

Figs. 20-21 - Intergranular crack propagation (SEM) along the direction of load application in 2090-T8E41.

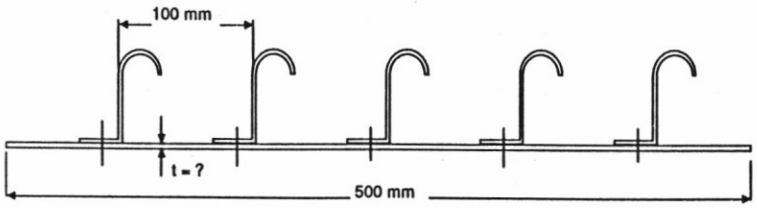

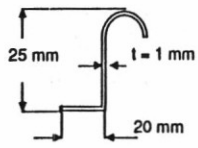

stringer area: 54 mm^2
rivet diameter: 3.18 mm
rivet pitch: 20 mm
rigid rivet behaviour

NDI ==> minimum inspectable crack length: 3 mm.

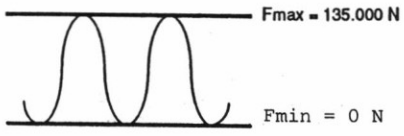

Each flight is equivalent, from the point of view of damage, to the two load cycles shown.

Fatigue Design Goals

Crack-free life : 20000 flights
Damage tolerance: the panel must sustain at least 10000 flights without failure under a Fail-Safe load of 225000 N (inspection interval: 5000 flights).

Fig. 22 - Simplifying assumptions made in the example of application of the data obtained.